Proceedings of the 7th International Conference on Mechanics and Materials in Design
Albufeira/Portugal 11-15 June 2017. Editors J.F. Silva Gomes and S.A. Meguid.
Publ. INEGI/FEUP (2017)

PAPER REF: 6847

LIMIT AND NON-LINEAR ANALYSIS OF A SLENDER ARCH BRIDGE. A COMPARATIVE STUDY

Elisa Conti[1(*)], Pier Giorgio Malerba[2], Manuel Quagliaroli[3]
[1]Department of Civil and Environmental Engineering, Politecnico di Milano, Milan, Italy
[2]Department of Civil and Environmental Engineering, Politecnico di Milano, Milan, Italy
[3]Structural Engineer at m[2]Structures, Piacenza, Italy
[(*)]*Email:* elisa.conti@polimi.it

ABSTRACT

A slender arch bridge has been studied by means of two approaches based on completely different assumptions: the Non Linear Analysis, suitable to represent the evolution of the structural behaviour in terms of both displacements and internal forces, all along the load path until the collapse, and the Limit Analysis, which highlights the mechanism of collapse and determines the ultimate value of the load multiplier. Within the limits of the two methodologies, the results are compared and discussed, outlining the effects on the numerical solutions of the concrete effectiveness factor and of the steel strain hardening.

Keywords: Arch bridge, Concrete structures, Limit analysis, Non Linear analysis.

INTRODUCTION

Modellization of Reinforced Concrete (R.C.) structures by means of beam elements is the most used tool of analysis in Civil Engineering design. For skeleton analyses the frame modellization perfectly fits the actual structure, but plane and spatial frames are used also to discretize continuous systems, like shear walls and bridge decks, made of orthotropic grillages. Frame analysis possesses many relevant characteristics. First of all, it is characterized by simplicity and geometrical effectiveness in modelling the actual structure. These properties make the planning of the analyses easy to do and simple to be verified. Moreover, it works through generalized stresses (i.e. axial force *N*, shear force *V*, bending moment *M* and torque moment *T*) and not with local stresses (σ_{ij}). Such synthetic representation of the internal stresses conforms to that, based on *N, V, M, T*, establishing the basic theory of the reinforced and prestressed concrete.

The *linear elastic analyses* (LEA) require only the modulus of elasticity and the gross dimensions of the member composing the skeleton. The resulting internal forces can be immediately used for proportioning the structural element, that is for refining the sectional dimensions and for computing the amount of the reinforcement.

In *non linear analyses* (NLA), both concrete and steel reinforcement contribute in defining the internal work which leads to the iterative research of the equilibrium. It gives in this way a more deepen assessment of the interaction mechanisms between concrete and steel reinforcement. Basic mechanisms are those based on axial-bending interaction only (Kang, 1980), (Bontempi, 1995), but there are beam elements based on more rich shape functions, which allow to take into account also the membrane effects and model the shear behavior (Bairan, 2007), (Quagliaroli, 2014). Many sorts of refinements to the frame analysis have

been reported in Literature, for instance to improve the modelling of cracking and deformability or to take into account bond-slip effects (Bontempi, 2000). Non Linear analyses require the material constitutive laws and a failure criterion, the dimensions and reinforcement of the member composing the structure and a loading history. The results allow a thorough description of the structural behavior (displacements and internal stresses, onset and conventional extension of cracking) and identify the ultimate load when the equilibrium is no longer satisfied. Of common interest are the load displacements curves of certain characteristic control nodes, which help to understand the behavior of the structure till the collapse.

A different tool to analyze the behavior of a framed structure and to assess its bearing capacity, determining the collapse load, is the *limit analysis* (LA), based on the plastic theory (Prager, 1955), (Dorn, 1957), (Massonnet, 1965), (Nielsen, 1984). Limit analysis works with rigid perfectly-plastic constitutive laws of the materials (concrete and steel) and requires the dimensions and reinforcement of the member composing the structure and a loading configuration, which can be composed of a fixed contribution and of a variable part, to be increased by a loading multiplier λ. The results are expressed in terms of the kinematic of the mechanism activated at the collapse (collapse mode) and of the collapse multiplier λ.

Hence, considering the same structure, the NLA represents the evolution of its behavior, in terms both of displacements and internal forces, all along the load path until the collapse. The LA highlights the mechanism of collapse as well as the axial force and bending moment distributions and determines the ultimate value of the load multiplier.

This paper, after short recalls of the essentials of Limit and Non Linear Analysis, studies with both the methods an existing R.C. slender arch bridge and compares the relevant results. Two aspects are highlighted: the complementary of the information given by the two methods (the load history versus the collapse mode) and the intensity of the ultimate loads. In an ideal comparison, the ultimate load given by the two different analyses is the only common and comparable result and one expects that, apart truncation and rounding approximations, it is unique. In truth, some differences may exist. The sources of these differences, referred to the case studied, are analyzed and discussed and may result a useful reference in approaching analogous problems.

A BRIEF RECALL OF A MATRIX APPROACH TO THE LIMIT ANALYSIS

The Limit Analysis of plane framed structures has been widely studied by many Authors. In particular, we refer to the formulation of the method presented in the works by (Martinez y Cabrera, 1977) and, recently, by (Biondini, 2008).

The axial force N and the bending moment M are the interacting generalized plastic stresses. Shear effects are neglected. Stresses and correlative generalized plastic strains, represented by the cross-sectional axial elongation Δl and bending rotation θ, are related by a rigid perfectly-plastic constitutive law Fig.1(a), (b). In this way, the behavior of the discrete cross-sections where the plastic strains tend to develop, can be represented by a generalized plastic hinge that allows a free axial-bending kinematic behavior and, at the same time, fully transfers the corresponding plastic values of the axial force and bending moment. Locus of the ultimate axial forces and bending moments is the frontier of the interaction domain associated to each section. We assume that the formation of plastic hinges occurs at the ends of the elements. The resulting approximations can be overcome by increasing the number of the elements.

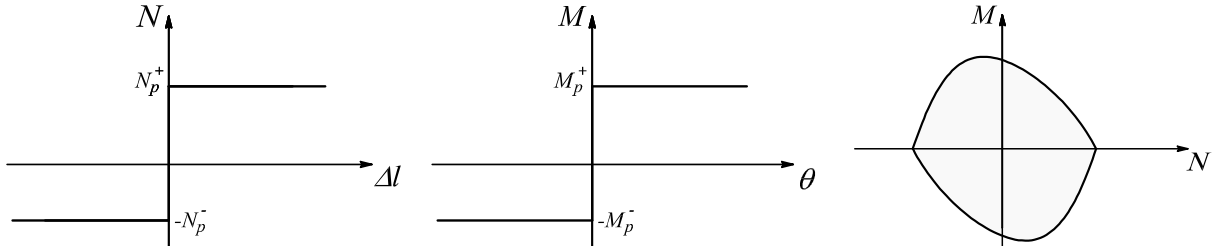

(a) Axial force - displacement. (b) Bending moment - rotation. (c) M-N domain.

Fig. 1 - Limit analysis hypotheses: rigid plastic constitutive law and M-N domain.

The plastic collapse is reached when the set of generalized plastic hinges allows the activation of a kinematic mechanism, for which the equilibrium can no longer be satisfied. In order to apply the two fundamental theorems of limit analysis, global equilibrium and compatibility equations are derived considering the generic structure of Fig.2(a) subdivided in finite elements as shown in Fig.2(b). End forces and generalized stresses of the beam element are assumed in accordance with the conventions and reference system shown in Fig.2(c). In the discretization, distributed loads are replaced by equivalent concentrated loads applied in an appropriate number of cross-sections. Finer mesh subdivisions can be introduced to increase the accuracy.

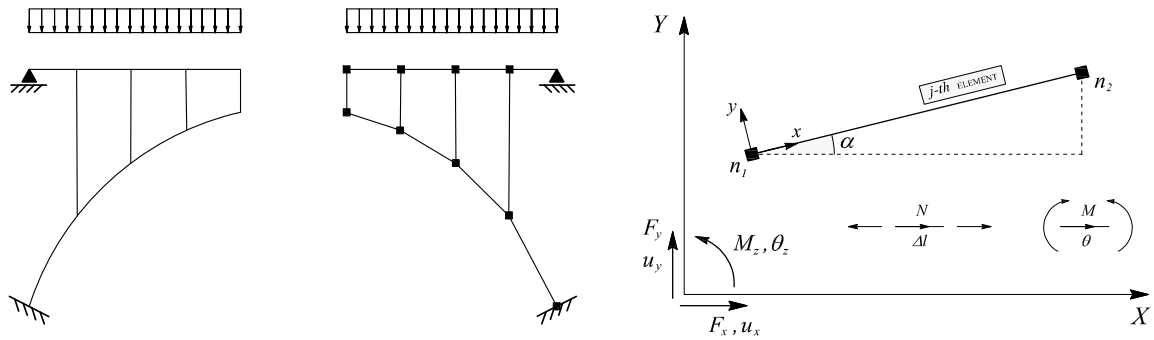

(a) Geometry. (b) Mesh. (c) Reference system.

Fig. 2 - Limit analysis: structural geometry, structural mesh and reference system.

Matrix Formulation.

For the generic *j-th* element of the structure, the equilibrium conditions are set in accordance to the force method. In the local coordinate system, shown in Fig.3(a), by removing the rigid body motions, the relationship between the internal forces $r_i = [N_i \quad M_i]^T$ at the sections ($x = 0; x = l_j$) and the basic forces $\bar{\mathbf{Q}}_j$ at the end nodes n_1, n_2 and that between the end global forces $\mathbf{Q}_j$ (Fig. 5(a)) and $\bar{\mathbf{Q}}_j$, are given, respectively, by the following equilibrium equations:

$$\begin{bmatrix} N_i \\ M_i \end{bmatrix} = \begin{bmatrix} 1 & 0 & 0 \\ 0 & (x/l-1) & x/l \end{bmatrix} \begin{bmatrix} \bar{Q}_1 \\ \bar{Q}_2 \\ \bar{Q}_3 \end{bmatrix} \tag{1}$$

$$\begin{bmatrix} Q_1 \\ Q_2 \\ Q_3 \\ Q_4 \\ Q_5 \\ Q_6 \end{bmatrix} = \begin{bmatrix} -1 & 0 & 0 \\ 0 & 1/l & 1/l \\ 0 & 1 & 0 \\ 1 & 0 & 0 \\ 0 & -1/l & -1/l \\ 0 & 0 & 1 \end{bmatrix} \begin{bmatrix} \bar{Q}_1 \\ \bar{Q}_2 \\ \bar{Q}_3 \end{bmatrix} \qquad \mathbf{Q}_j = \mathbf{h}_l \bar{\mathbf{Q}}_j \tag{2}$$

By introducing the transformation matrix $\mathbf{T}_\alpha$:

$$\mathbf{T}_\alpha = \begin{bmatrix} \mathbf{T}_0 & \mathbf{0} \\ \mathbf{0} & \mathbf{T}_0 \end{bmatrix} \qquad \text{with} \qquad \mathbf{T}_0 = \begin{bmatrix} \cos\alpha & -\sin\alpha & 0 \\ \sin\alpha & \cos\alpha & 0 \\ 0 & 0 & 1 \end{bmatrix} \tag{3}$$

we derive the nodal forces in the global reference system $\mathbf{Q}_{g,j}$ from the local ones $\mathbf{Q}_j$, through the relationship:

$$\mathbf{Q}_{g,j} = \mathbf{T}_\alpha \mathbf{Q}_j \qquad \mathbf{Q}_{g,j} = (\mathbf{T}_\alpha \mathbf{h}_l) \cdot \bar{\mathbf{Q}}_j = \mathbf{H}_{g,j} \cdot \bar{\mathbf{Q}}_j \tag{4}$$

where $\mathbf{H}_{g,j}$ is the transformed equilibrium matrix, for the *j-th* element.

By assembling over all the *ne* elements, we obtain the global equilibrium equations which correlate the vector $\mathbf{Q}_t$, containing all the element basic forces, to the external nodal forces vector $\mathbf{F}_e$, by means of the equilibrium matrix $\mathbf{H}$ of the whole structure, derived as follows:

$$\mathbf{F}_e = \sum_{j=1}^{ne} \mathcal{A}(\mathbf{Q}_{g,j}) = \sum_{j=1}^{ne} \mathcal{A}(\mathbf{H}_{g,j} \cdot \bar{\mathbf{Q}}_j) = \mathbf{H} \cdot \mathbf{Q}_t \tag{5}$$

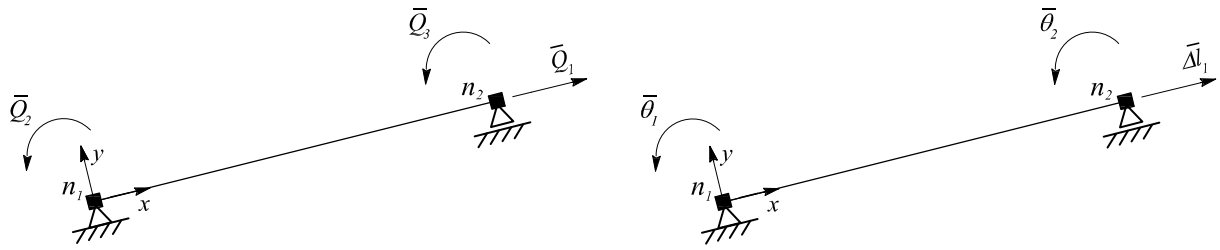

(a) Basic forces - Static field. (b) Basic displacement - Kinematic field.

Fig. 3 - Static and Kinematic field: element without rigid body modes.

Compatibility conditions are derived through the Virtual Force Principle, by equating the virtual internal work $\delta W_i = \delta \mathbf{Q}_t^T \mathbf{q}_t$ and external one $\delta W_e = \delta \mathbf{F}_e{}^T \mathbf{s}$. From Eq.(5), we have $\delta \mathbf{F}_e = \mathbf{H} \delta \mathbf{Q}_t$ and stating $\delta W_e = \delta W_i$, we obtain:

$$\delta \mathbf{Q}_t^T \mathbf{H}^T \mathbf{s} = \delta \mathbf{Q}_t^T \mathbf{q}_t \tag{6}$$

Since such an equation is valid for any choice of $\delta \mathbf{Q}_t^T$, the compatibility equations are finally obtained:

$$\mathbf{q}_t = \mathbf{H}^T \cdot \mathbf{s} \tag{7}$$

The compatibility matrix $\mathbf{H}^T$ is the transposed of the equilibrium matrix $\mathbf{H}$. In these correspondences, the vector of the forces $\mathbf{F}_e$ works for that of the displacements $\mathbf{s}$ in the global reference system, as the vector of the basic forces $\mathbf{Q}_t$ works for that of the basic displacements $\mathbf{q}_t$ (Fig.3(b)).

Basic hypotheses. Yield Condition. Flow Rule.

We assume that before the collapse the displacements are small and the structure is stable. Limit analysis considers materials modelled through rigid perfectly-plastic constitutive laws. The material behavior is defined through the following two conditions:

(a) a yielding criterion, which defines the stress state corresponding to the start of the plastic flow. The yield function must be convex.

(b) the flow rule, which correlates the increments of the plastic strains to the actual stress state. The flow rule is associated to the yielding surface (normality rule).

In the present case, where the only active generalized plastic stresses for the *i-th* critical cross section are the axial force N_i and the bending moment M_i, the yielding criterion has the shape shown in Fig.1(c), which can be defined by the equation $f_i(N_i, M_i) = 0$. The stress state must verify the condition $f_i(N_i, M_i) \le 0$. The frontier of such a domain can be reasonably idealized by a stepwise approximation. Adopting a conservative approach, the stepwise frontier is assumed inscribed within the actual one. By assuming a stepwise linearization with q sides, for each *i-th* plastic domain (Fig.4), the yielding criterion for the *i-th* critical cross section may be written in matrix form as follows:

$$\mathbf{\Phi}_i = \mathbf{N}_i \mathbf{r}_i - \mathbf{k}_i \le 0 \tag{8}$$

where: $\mathbf{\Phi}_i = \begin{bmatrix} \phi_1^i & \phi_2^i & \dots & \phi_{q_i}^i \end{bmatrix}^T$, $\mathbf{N}_i = \begin{bmatrix} \mathbf{n}_1^i & \mathbf{n}_2^i & \dots & \mathbf{n}_{q_i}^i \end{bmatrix}^T$, $\mathbf{n}_j^i = \begin{bmatrix} n_{j1}^i & n_{j2}^i \end{bmatrix}^T$,

$\mathbf{k}_i = \begin{bmatrix} k_1^i & k_2^i & \dots & k_{q_i}^i \end{bmatrix}^T \ge \mathbf{0}$

For each element and, assembling these conditions for the whole structure, the yield criterion becomes:

$$\mathbf{\Phi}_i = \mathbf{N}_i \bar{\mathbf{Q}}_i - \mathbf{k}_i \le 0 \qquad \Rightarrow \qquad \mathbf{\Phi}_t = \sum_{j=1}^{ne} A(\mathbf{\Phi}_j) = \mathbf{N}\mathbf{Q}_t - \mathbf{k} \le 0 \tag{9}$$

The associated flow rule for *i-th* critical cross-section is given by the equations:

$$\mathbf{d}_i = \begin{cases} \Delta l_i & = \mu_i \dfrac{\partial f_i}{\partial N_i} \\ \theta_i & = \mu_i \dfrac{\partial f_i}{\partial M_i} \end{cases} \tag{10}$$

where $\mathbf{d}_i$ is the vector of plastic strains, normal in each point to the frontier and $\mu_i \ge 0$ is the multiplier that allows plastic flows only for the points lying on the yielding curve, for which the normal is oriented outside the domain, that is $\mu_i f_i(n_i, m_i) = 0$. For the linearized case with q sides, by introducing the vector $\boldsymbol{\mu}_i = \begin{bmatrix} \mu_1^i & \mu_2^i & \dots & \mu_q^i \end{bmatrix}^T$ collecting the terms μ_i^j relative to each side of the linearized frontier, the following notation is derived:

$$\mathbf{d}_i = \mathbf{N}_i^T \cdot \boldsymbol{\mu}_i \qquad \text{with} \qquad \begin{cases} \mu_j^i \cdot \phi_j^i = 0 & j = 1, \cdots, q \\ \boldsymbol{\mu}_i > 0 \end{cases} \tag{11}$$

The flow rule can be written for the generic element by connecting the vector of plastic strain $\mathbf{d}_i$ with the vector of basic displacement $\bar{\mathbf{q}}$ by means of the compatibility equations.

$$\bar{\mathbf{q}} = \mathbf{N}_i^T \cdot \boldsymbol{\mu}_i \tag{12}$$

By assembling all the element contributions for the entire structure:

$$\mathbf{q} = \sum_{j=1}^{ne} A(\bar{\mathbf{q}}_j) = \mathbf{N}^T \cdot \boldsymbol{\mu} \quad \text{with} \quad \begin{cases} \mu_j^i \cdot \phi_j^i = 0 & j = 1, \cdots, q \\ \boldsymbol{\mu} > 0 \end{cases} \tag{13}$$

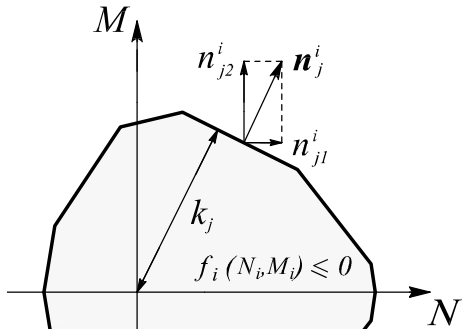

Fig. 4 - Linearized plastic domain. Yield criterion and normality rule.

The static and the kinematic approach.

With reference to a generic structure, let $\mathbf{P}_0$ be a vector of constant loads and $\mathbf{P}$ a vector of loads whose intensity varies proportionally to a unique multiplier $\lambda \geq 0$. We assume that for $\lambda = 0$, equilibrium and compatibility are satisfied. We search for the multiplier λ_c associated to the collapse load (*collapse multiplier*).

On the basis of the two fundamental theorems of limit analysis, we can restate the limit analysis as a problem of linear mathematical programming. In mathematical terms, the upper and lower bound theorems are traduced in the following dual linear constrained optimization problems, solved here by means of the Simplex Method.

Lower bound theorem:

$$\lambda_c = \max\left\{\lambda \;\; | \;\; \lambda\mathbf{P} - \mathbf{H}\mathbf{Q}_t = -\mathbf{P}_0, \quad \mathbf{N}\mathbf{Q}_t \leq \mathbf{k}, \quad \lambda \geq 0\right\} \tag{14}$$

Upper bound theorem:

$$\lambda_c = min\left\{\mathbf{k}^T\boldsymbol{\mu} - \mathbf{P}_0^T\mathbf{s} \;\; | \;\; \mathbf{N}^T\boldsymbol{\mu} - \mathbf{H}^T\mathbf{s} = \mathbf{0}, \quad \mathbf{P}^T\mathbf{s} = 1, \quad \mu \geq 0\right\} \tag{15}$$

In this way, Eq.(14) requires finding a maximum multiplier, while Eq.(15) a minimum one. It must be outlined that in the second case, the minimum condition is related to the work done by the proportional loads $\mathbf{P}$ for the displacements $\mathbf{s}$ associated with the collapse mechanism. Since this mechanism is correlated to an arbitrary multiplier, it results univocally identified by the condition $\mathbf{P}^T\mathbf{s} = 1$. As known, the uniqueness of λ_c does not necessarily mean the uniqueness of the collapse mechanism, or that of the stress field at collapse.

A BRIEF RECALL OF NON-LINEAR ANALYSIS WITH R.C. BEAMS ELEMENTS

The non-linear analysis is based on a special type of R.C. beam element previously formulated by Bontempi and Malerba (Bontempi, 1995), (Bontempi, 1997), (Martinez y Cabrera, 1997).

According to the Bernoulli-Navier theory, we assume that any beam section rotates remaining plane. At the section of abscissa $(0 \le x \le l)$, the axial and transversal displacements $\mathbf{u} = [u_0(x) \quad v_0(x)]^T$ depend on the nodal displacement $\mathbf{q}^T = [q_1 \ q_2 \ q_3 \ q_4 \ q_5 \ q_6]^{\mathrm{T}}$ by means of the following equation:

$$\mathbf{u}(x) = \begin{bmatrix} N_1(x) & 0 & 0 & N_4(x) & 0 & 0 \\ 0 & N_2(x) & N_3(x) & 0 & N_5(x) & N_6(x) \end{bmatrix} \mathbf{q} = \begin{bmatrix} \mathbf{N}_a & \mathbf{0} \\ \mathbf{0} & \mathbf{N}_b \end{bmatrix} \mathbf{q} = \mathbf{N}(x)\mathbf{q} \tag{16}$$

where $\mathbf{N}(x)$ is a matrix of displacement functions, usually based on cubic Hermitian polynomials for the transverse displacement fields $\mathbf{N}_b$ and linear Lagrangian shape functions for the axial displacement $\mathbf{N}_a$.

The generalized strains are the axial elongation and the curvature $\mathbf{e}_{\mathrm{s}}(x) = [\varepsilon_0(x) \quad \chi(x)]^T$, derived from Eq.(16), by means of the following relationship:

$$\mathbf{e}_{\mathrm{s}}(x) = \begin{bmatrix} \dfrac{\partial \mathbf{N}_a}{\partial x} & \mathbf{0} \\ \mathbf{0} & \dfrac{\partial^2 \mathbf{N}_b}{\partial x^2} \end{bmatrix} = \begin{bmatrix} N_{1,x} & 0 & 0 & N_{4,x} & 0 & 0 \\ 0 & N_{2,xx} & N_{3,xx} & 0 & N_{5,xx} & N_{6,xx} \end{bmatrix} \mathbf{q} = \mathbf{B}(x)\mathbf{q} \tag{17}$$

In the same section, the normal strain $\varepsilon_x = \varepsilon_x(x, y)$ at a fiber at the distance y from the beam axis is given by:

$$\varepsilon_x = \mathbf{a}_s^T \mathbf{e}_s(x) = \mathbf{a}_s^T \mathbf{B}(x)\mathbf{q} \quad \text{with} \quad \mathbf{a}_s = [1 \quad -y] \tag{18}$$

Through the Principle of Virtual Displacements, we state that the virtual internal work δW_i equals the external one δW_{e}, due to:

(a) the distributed applied loads acting along the axis of the beam $\mathbf{f}_p = [p_x \ \ p_y]^T$;

(b) the forces directly applied at the nodes $\mathbf{f}_n = [F_{xi} \ \ F_{yi} \ \ M_i \ \ F_{xj} \ \ F_{yj} \ \ M_j]^T$;

(c) the end forces through which the beam interacts with the rest of the structure $\mathbf{f}_q = [Q_1 \ \ Q_2 \ \ Q_3 \ \ Q_4 \ \ Q_5 \ \ Q_6]^T$.

For a virtual displacement $\delta\mathbf{q}$, the virtual external work δW_{e} is:

$$\begin{aligned} \delta W_{\mathrm{e}} &= \int_0^l \delta\mathbf{u}^T(x) \cdot \mathbf{f}_p(x)dx + \delta\mathbf{q}^T \cdot \mathbf{f}_n + \delta\mathbf{q}^T \cdot \mathbf{f}_q = \\ &= \int_0^l \delta\mathbf{q}^T \mathbf{N}^T(x) \cdot \mathbf{f}_p(x)dx + \delta\mathbf{q}^T \cdot \mathbf{f}_n + \delta\mathbf{q}^T \cdot \mathbf{f}_q = \\ &= \delta\mathbf{q}^T \left[\mathbf{f}_{ne} + \mathbf{f}_n + \mathbf{f}_q \right] \end{aligned} \tag{19}$$

where $\mathbf{f}_{ne}$ are the equivalent nodal forces. For a virtual displacement $\delta\mathbf{q}$, the corresponding virtual strain is $\delta\varepsilon_x = \mathbf{a}_s^T \cdot \delta\mathbf{e}_s(x) = \mathbf{a}_s^T \mathbf{B}(x) \cdot \delta\mathbf{q}$ and the virtual internal work δW_i results:

$$\begin{aligned}\delta W_i &= \int_V \delta\varepsilon_x^T(x,y)\cdot\sigma_x(x,y)dV = \int_V \delta\mathbf{e}_s^T(x)\mathbf{a}_s^T(y)\cdot\sigma_x(x,y)dV = \\ &= \int_0^l \delta\mathbf{e}_s^T(x)\left(\int_A \mathbf{a}_s^T(y)\cdot\sigma_x(x,y)dA\right)dx = \int_0^l \delta\mathbf{e}_s^T(x)\cdot\mathbf{f}_s(x)dx = \\ &= \int_0^l \delta\mathbf{q}^T\mathbf{B}^T(x)\cdot\mathbf{f}_s(x)dx = \delta\mathbf{q}^T\int_0^l \mathbf{B}^T(x)\cdot\mathbf{f}_s(x)dx = \delta\mathbf{q}^T\cdot\mathbf{f}_q\end{aligned} \tag{20}$$

where $\mathbf{f}_s(x) = \begin{bmatrix} N & M \end{bmatrix}^T = \int_A \mathbf{a}_s^T(y)\cdot\sigma_x(x,y)dA$ are the section restoring forces and $\mathbf{f}_q$ the element restoring forces as reported in Fig.5(a).

$$\mathbf{f}_q = \int_0^l \mathbf{B}^T(x)\cdot\mathbf{f}_s(x)dx = \left[\int_0^l \mathbf{B}^T(x)\cdot\mathbf{k}_s(x)\cdot\mathbf{B}(x)dx\right]\cdot\mathbf{q} = \mathbf{k}_e\cdot\mathbf{q} \tag{21}$$

The element stiffness matrix $\mathbf{k}_e = \int_0^l \mathbf{B}^T(x)\cdot\mathbf{k}_s(x)\cdot\mathbf{B}(x)dx$ is function of the stiffness matrix $\mathbf{k}_s(x)$ of the section at the abscissa *x*. The matrix $\mathbf{k}_s$ is computed for each section by integration over the area of the composite element and by assembling the contributes of concrete and steel. In order to deal with sections of arbitrary shape, the generic cross-section is divided into subdomains. Through a parametric transformation of each subdomain into a unit square parent domain, Gaussian integration rules can be carried out with several integration strategies, as shown in Fig.6 (Quagliaroli, 2015). The so-called "fiber method" is a particular case of these integration procedures.

Relating these quantities to the global reference system and by assembling the equilibrium equation of the whole structure the following relationship is obtained:

$$\mathbf{K}\cdot\mathbf{s} = \mathbf{f} \tag{22}$$

where $\mathbf{K}$ is the assembled stiffness matrix, $\mathbf{s}$ the unknown displacements of the whole structure and $\mathbf{f}$ the vector of the applied loads. The nonlinear system in Eq.(22) is solved through a secant approach, with the following convergence criteria.

(a) Displacement criterion

$$\left\|\frac{\mathbf{s}^i - \mathbf{s}^{i-1}}{\mathbf{s}^i}\right\| \le toll_1 \tag{23}$$

(b) Energy criterion

$$\left|\frac{\mathbf{s}^i\cdot(\mathbf{f}(\mathbf{s}^i) - \mathbf{f}_r(\mathbf{s}^i))}{\mathbf{s}^i\cdot\mathbf{f}_r(\mathbf{s}^i)}\right| \le toll_2 \tag{24}$$

(c) Out-of-balance load criterion

$$\left\|\mathbf{f}(\mathbf{s}^i) - \mathbf{f}_r(\mathbf{s}^i)\right\| \le toll_3 \tag{25}$$

where $\mathbf{f}_r$ is the vector of the assembled restoring forces. At the end of each iteration, the solution obtained should be checked to see whether it has converged within preset tolerances. This iterative procedure continues until one of this state is achieved:

1. Equilibrium between internal and external forces is guaranteed.
2. Strain in concrete or steel reaches the limit value (collapse of the corresponding section occurs).
3. Loss of equilibrium, since the reactions request for the applied loads $\mathbf{f}$ can no longer be developed.

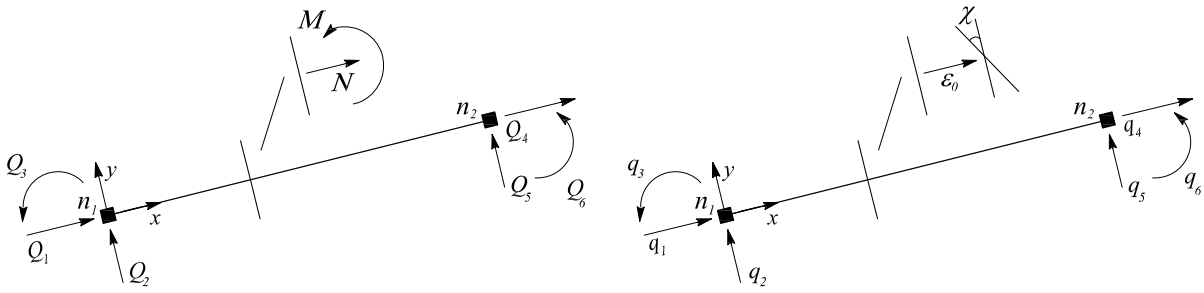

(a) Static quantities. (b) Kinematic quantities.

Fig. 5 - Beam element notations. Static and kinematic fields.

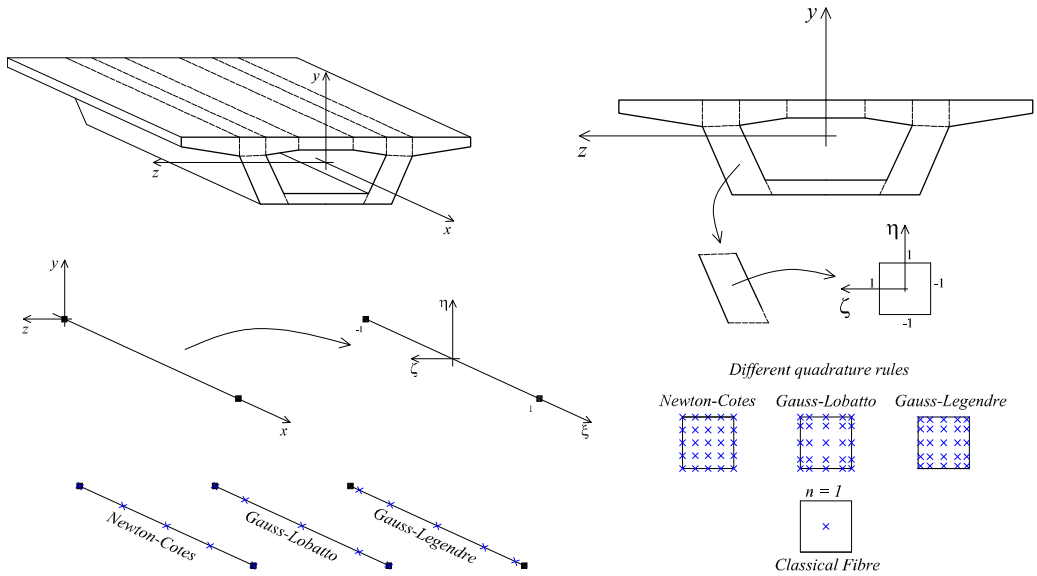

Fig. 6 - Integration strategies on the beam element (left side) and on the section (right side). The section is divided into sub-domains and the integration works sampling in a parent domain by using parametric transformations. The so called "fiber approach" is a particular case of these integration procedures.

APPLICATION TO A SLENDER ARCH BRIDGE

Structure, materials and loads.

A R.C. slender arch bridge, crossing the Corace River (Gimigliano, Cosenza, Italy, 1955), is studied (Galli, 1985). The arch has a span l = 80 m and a rise f = 26.10 m. At platform level the total height is h = 27.00 m. Fig.7 shows the bridge geometry. Table 1 summarises the overall dimensions and Table 2 reports the nodal coordinates of the left half of the arch. Eight internal columns subdivide the upper girder into nine segments each with a different reinforcement. Table 3 lists the type and the total amount of bars of each segment. Table 4 lists the reinforcement characteristics of the arch segments and of the columns.

As concerns the material characteristics, in the Non Linear Analysis, concrete is modelled by a no-tension uniaxial stress-strain law, according to Sargin formulation. The design compression strength is $f_c = -30\ MPa$, with a transition strain $\varepsilon_{c0} = -0.002$ and an ultimate strain $\varepsilon_{cu} = -0.0035$. The steel is described by an bilinear stress-strain diagram, symmetric both in tension and compression, with a yielding stress $f_{sy} = 300\ MPa$, elastic modulus $E_s = 206000\ MPa$, hardening modulus $E_h = 4100\ MPa$ (E_h/E_s □ 0,2) and ultimate limit

strain $\varepsilon_{su} = 0.010$. In the Limit Analysis, only the concrete compression strength and the steel yielding stress are involved. Table 5 summarises the material properties.

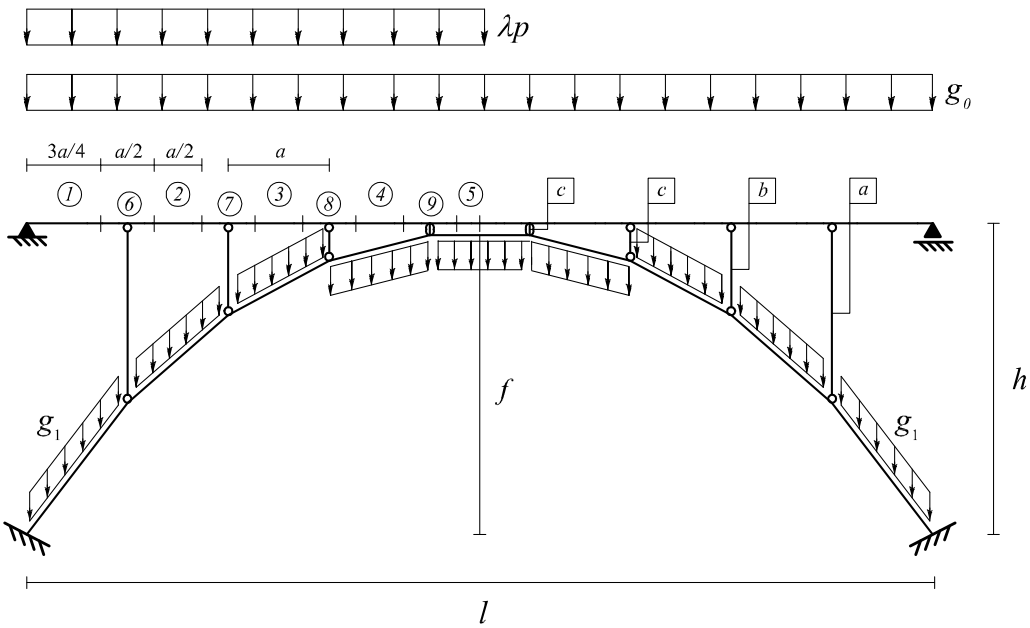

Fig. 7 - Corace Bridge. Geometric characteristics and loading condition. The encircled numbers identify the different reinforcement of the sections distribution along the beam. The letters inclosed in squares identify the section type of the columns.

Table 1 - Overall dimension.

l	80.00	m
f	26.10	m
h	27.00	m
g_0	102.9	kN/m
g_1	85.0	kN/m
p	53.3	kN/m

Table 2 - Nodal coordinates of the arch left half.

x [m]	*y [m]*
0.00	0.00
8.89	11.43
17.80	19.04
26.70	23.76
35.60	25.98
40.00	26.10

Table 3 - Top A_S' $[mm^2]$ and bottom A_S $[mm^2]$ reinforcements for different segments of the upper girder.

Girder	1	2	3	4	5	6	7	8	9
A_S'	19465.31	36090.62	32396.10	25007.08	21312.56	36090.02	36090.62	34243.36	26854.33
A_S	12930.80	18472.56	25861.59	14778.05	14778.05	12930.80	22167.08	16625.31	14778.05

Table 4 - Reinforcement distribution in the arch and in the columns.

Element	Arch	Column Type A	Column Type B	Column Type C
A_S'	27708.85	3053.63	3053.63	3053.63
A_S	27708.85	3053.63	3053.63	3053.63

Table 5 - Material characteristics assumed in the constitutive law.

Concrete	$f_c = 30\ MPa$	$\varepsilon_{cu} = -0.0035$	$\varepsilon_{c0} = -0.002$	
Ordinary Steel	$f_{sy} = 300\ MPa$	$\varepsilon_{su} = 0.01$	$E_s = 206000\ MPa$	$E_h = 4100\ MPa$

The applied load is composed of a fixed contribution, corresponding to the dead loads of the girder ($g_0 = 102.90\ kN/m$) and of the arch ($g_1 = 85.00\ kN/m$), and of a variable part, corresponding to the live load ($p = 53.30\ kN/m$), to be increased until to the collapse. With reference to this structure, both Non Linear and Limit analyses have been carried out.

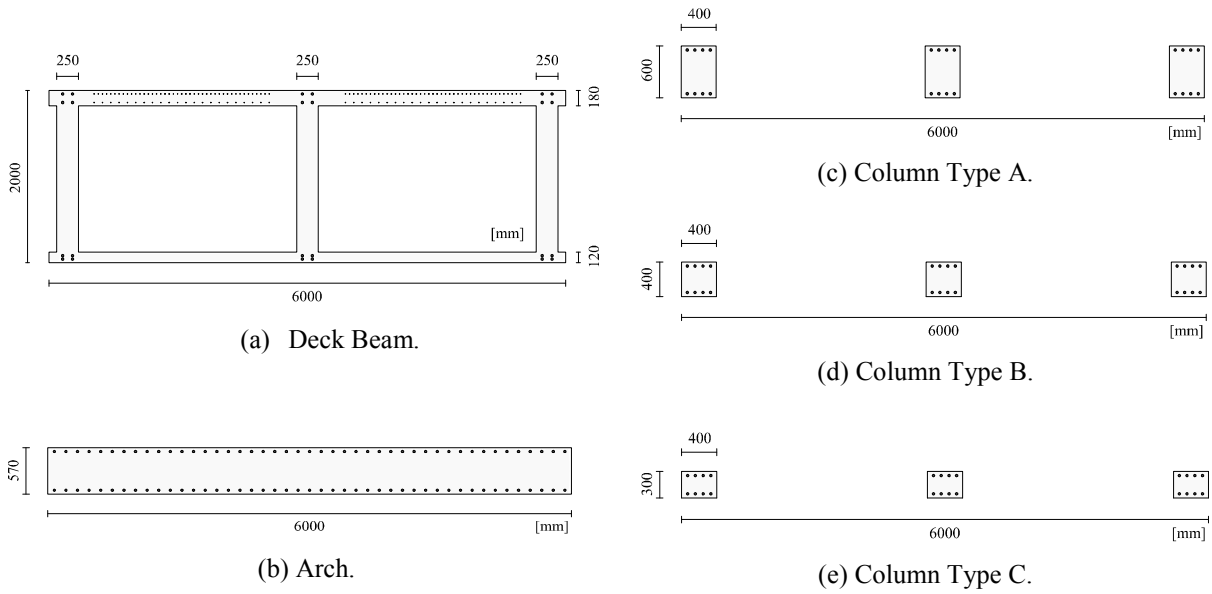

Fig. 8 - Corace Bridge. Geometry and reinforcement of the characteristic sections: (a) Girder; (b) Arch; (c) Column Type A; (d) Column Type B; (e) Column Type C.

Main results of the analyses.

Fig.9 shows the progressive evolution of the deformed shapes obtained from the step-by-step Non Linear Analysis for the live loading levels equal to 0%, 10%, 50%, 90% of the collapse load. Fig.10 shows the axial force and bending moment distributions just before the collapse.

Table 6 - Collapse loads resulting from Limit and Non Linear Analyses.

		Collapse Load p	Load Factor λ
Non Linear Analysis	(NLA)	214 kN/m	4.01
Limit Analysis	(LA)	217 kN/m	4.08

The results of the Limit Analysis are reported in Fig.11 and Fig.12. Figs.11(a), (b) show the axial force and bending moment distributions at incipient collapse. The lower bound theorem predicts the formation of the twelve plastic hinges, shown in Fig.12. on the scheme which presents the collapse mechanism of the structure. Figs.12(b), (c), (d), (e) show the points representing the ultimate values of the internal forces *N* and *M* on the linearized frontiers of

the most relevant sections corresponding to plastic hinges in the arch and in the upper girder. The collapse loads, derived from both analyses, are reported in Table 6.

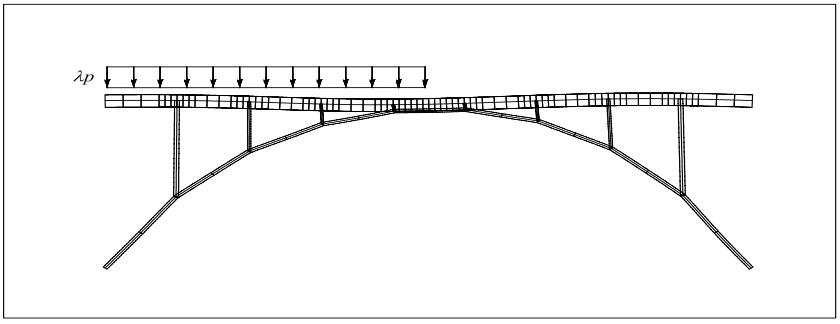

(a) Step 0. $g+\lambda p$; $\lambda=0\%$ of the collapse load.

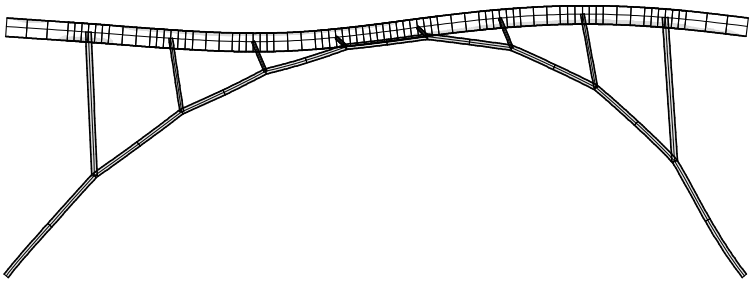

(b) Step 1. $g+\lambda p$; $\lambda=10\%$ of the collapse load.

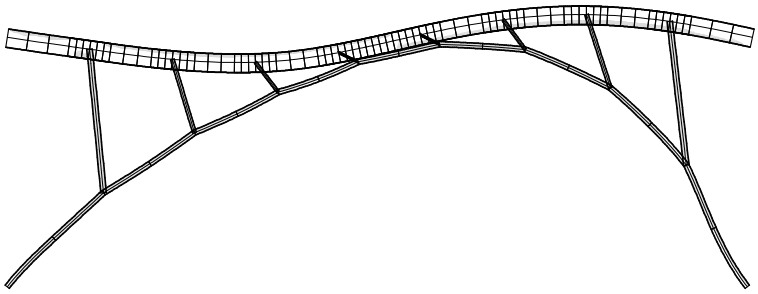

(c) Step 2. $g+\lambda p$; $\lambda=50\%$ of the collapse load.

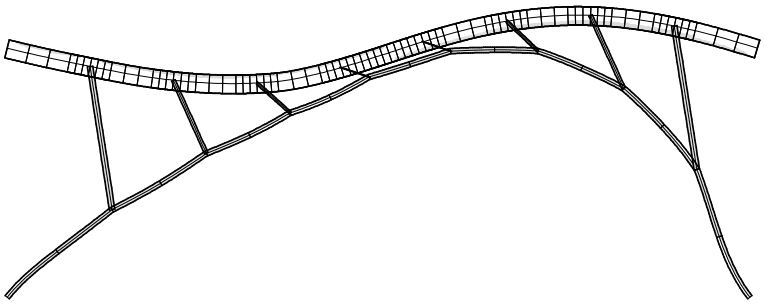

(d) Step 3. $g+\lambda p$; λ=90% of the collapse load.

Fig. 9 - Non Linear Analysis. Progressive evolution of the deformed configurations obtained by increasing the live load p until the collapse load is reached.

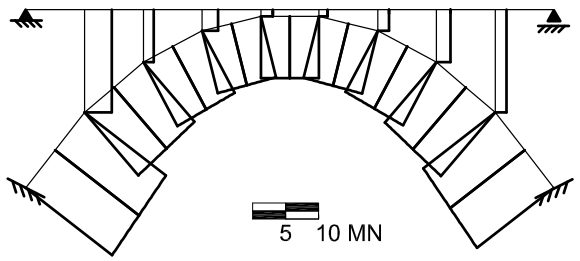

(a) Axial Force.

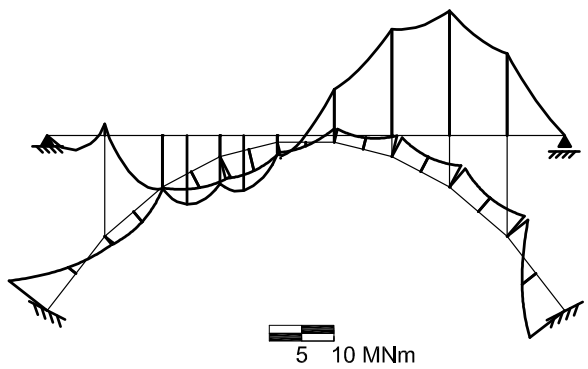

(b) Bending Moment.

Fig. 10 - Non Linear Analysis. Internal stresses *N* and *M* just before the live load *p* equals the collapse.

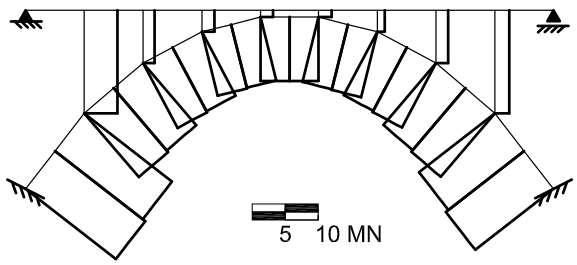

(a) Axial Force.

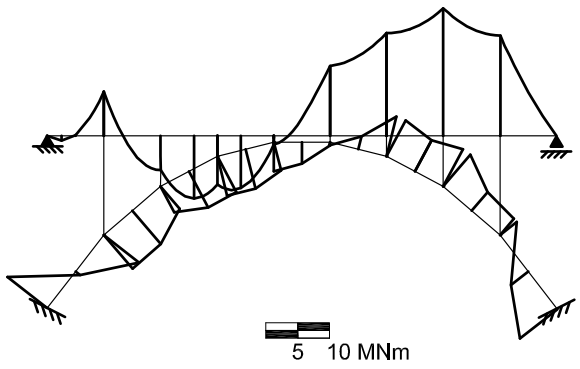

(b) Bending Moment.

Fig. 11 - Limit Analysis. Internal stresses *N* and *M* at the collapse load.

Analysis and comments of the results

A slender arch bridge has been studied by means of two approaches based on completely different assumptions: the NLA represents the evolution of the structural behavior in terms both of displacements and internal forces, all along the load path until the collapse; the LA highlights the mechanism of collapse and determines the ultimate value of the load multiplier. A comparison is possible in terms of the global response of the structure, but a direct comparison of numerical quantities is not possible.

In effect, the deformed shape of the structure at the incipient collapse given by the NLA (Fig.9) agrees with the shape of the collapse mechanism given by the LA (Fig.12(a)) and the location of the main plastic hinges well corresponds to that of the most stressed sections according to NLA. There is also a good correspondence between the axial force and bending moment distributions at incipient collapse and between the intensities of the collapse loads, as shown in Table 7.

Table 7 - Comparisons between Limit and Non Linear Analyses.

Limit Analysis	Collapse Load	Non Linear Analysis	Collapse Load Load p
Limit Analysis without effectiveness factor	217 kN/m	*Non Linear Analysis with elastic hardening steel behaviour*	214 kN/m
Limit Analysis with effectiveness factor	210 kN/m	*Non Linear Analysis with elastic perfectly plastic steel behaviour*	157 kN/m

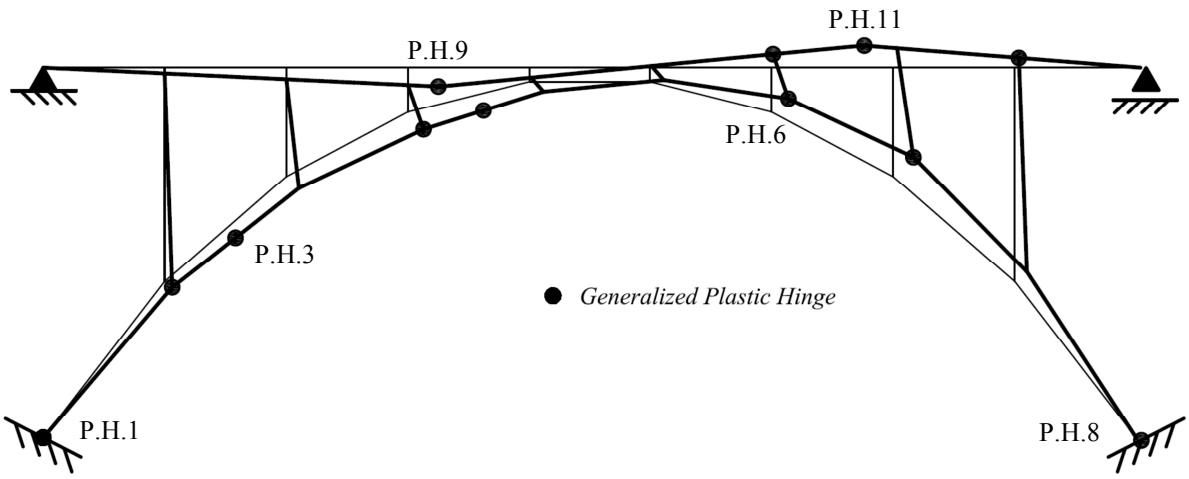

(a) Collapse mechanism (λ=4.08).

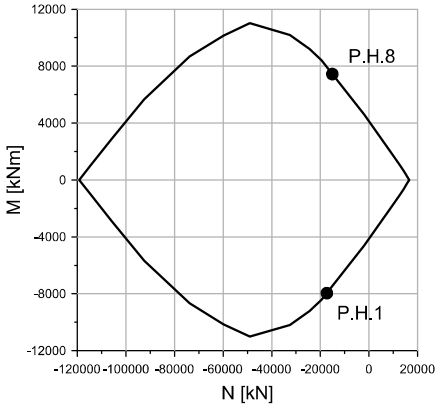

(b) Arch.

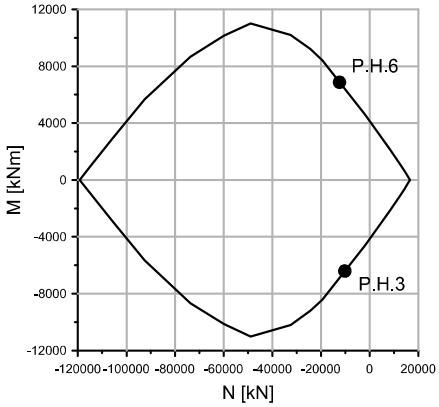

(c) Arch.

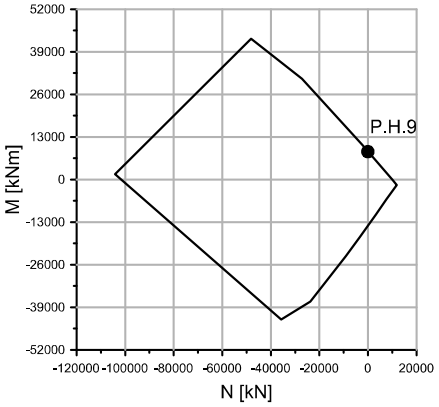

(d) Girder - Segment 4.

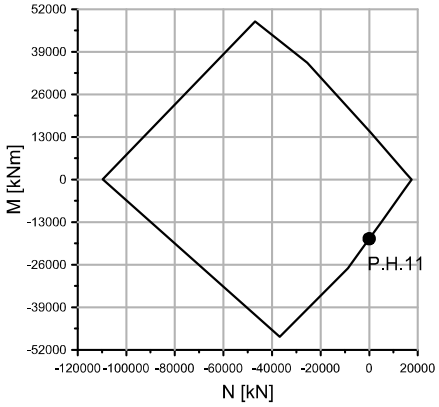

(e) Girder - Segment 3.

Fig. 12 - Limit Analysis. (a) Distribution of the plastic hinges which transform the structure into a mechanism. (b÷e) Points representing the ultimate values of the internal forces *N* and *M* on the linearized frontiers of the most relevant sections corresponding to plastic hinges in the arch and in the upper girder.

Comments on the results

These results were obtained after a set of comparative studies, which started from an initial response, very similar to that just exposed. The only difference was the use of an elastic perfectly plastic steel behaviour ($E_h/E_s = 0$), which led to an ultimate load $p_{NLA} = 157\,kN/m$ versus $p_{LA} = 217\,kN/m$. Such a difference may be explained as follows.

First of all, the Limit Analysis is based on the radical assumption that a material maintains its maximum stress level for strains of arbitrary magnitude (infinite ductility) and on the application of the normality criterion. It follows that these assumptions lead to overestimate the load carrying capacity. In order to take into account the fact that the assumptions of the LA are not always and fully satisfied when applied to reinforced concrete structures, many Authors (Exner, 1979), (Nilsen, 1984) suggest the introduction of a corrective effectiveness factor ($\nu_e \leq 1$), which factorizes the characteristic concrete strength before its use for the calculation of the carrying capacity of a structure. Design standards and literature suggest as conservative value $\nu_e = 0.85 - f_c/300$, which, for $f_c = 30\,N/mm^2$, results $\nu_e = 0.75$. By using such a reduction factor, the Limit Analysis gave as ultimate load $p_{LA} = 210\,kN/m$, equivalent to (-3.2%) with respect the initial one. Such negligible difference is fully justified. The effectiveness factor plays a crucial role in defining the bearing capacity of highly compressed concrete zones, like the stress block in bending, the struts of the shear mechanisms or the struts of a strut and tie model. In the present case, all the sections have a low degree of reinforcement and the collapse is driven by the yielding the steel.

On the other side, in the evolutive Non Linear Analysis the ultimate load is that for which the model reaches for the last time an equilibrium configuration, without violating the convergence conditions. This depends on the degree of refinement of the structural discretization and on the level of the loading increments at high level of the strains. The last iterations struggle to converge and usually lead to underestimate the ultimate load. In fact, if the steel strain hardens soon after the onset of yielding, the elastic perfectly plastic law leads to underestimate the steel stress at high strains (Park, 1975). The introduction of a light hardening property in the steel constitutive law, in this case $E_h/E_s \approx 0.02$, contributes in stabilizing and in extending the solution. As noted by Kappos (Kappos, 1997), the steel strain hardening better describes the behaviour of plastic hinge zones, since it allows the development of bending moments higher than those corresponding to first yielding at sections beyond the critical one, spreading of a plastic mechanism in larger parts of the member. Such a choice stabilizes the solution and, as shown, allows a better comparison between the two sets of results.

From the computational point of view, it would be appropriate to dedicate a future research to the study of the effects of light strain hardening of the steel on the structural response in the area immediately before the collapse.

CONCLUSIONS

After short recalls of the essentials of Non Linear and Limit Analysis, this paper studies an existing R.C. slender arch bridge with both methods and compares the most important results. Two aspects are highlighted: the complementarity of the information given by the two methods (the load history versus the collapse mode) and the intensity of the ultimate loads. In an ideal comparison, the ultimate load provided by the two different analyses is the only common and comparable result and, apart from truncation and rounding approximations, one expects this value to be unique. Actually, some differences may exist. Within the limits of the two methodologies, the results are compared and discussed, outlining the effects on the numerical solutions of the concrete effectiveness factor and of the steel strain hardening.

REFERENCES

[1]-Bairan JM, Mari AR. Multiaxial-coupled analysis of RC cross-sections subjected to combined forces. Engineering structures 29.8, 2007, 1722-1738.

[2]-Biondini F, Frangopol DM. Probabilistic limit analysis and lifetime prediction of concrete structures. Structure and Infrastructure Engineering, 2008, 399-412.

[3]-Bontempi F, Malerba PG, Romano L. Direct Non Linear Secant Analysis of R.C. and P.C. frames. Studies and Researches, Vol.16, F.lli Pesenti School, Politecnico di Milano, 1995.

[4]-Bontempi F, Malerba PG. The Role of Softening in the Numerical Non-Linear Analysis of Reinforced Concrete Frames. Selected paper for Structural Engineering and Mechanics, 1997.

[5]-Bontempi F, Malerba PG, Biondini F. Bond slip modelling in R.C. beam elements. 13° CTE Congress (Precast Technician Association Congress), Pisa, 09-11 November 2000, 125-134.

[6]-Dorn WS, Greenberg HJ. Linear programming and plastic limit analysis of structures. Quarterly of Applied Mathematics 15.2, 1957, 155-167.

[7]-Exner H. On the Effectiveness Factor in Plastic Analysis of Concrete. Plasticity in Reinforced Concrete. IABSE Colloqium, Copenhagen, 1979, 29, 35-42.

[8]-Galli A, Franciosi V. Il calcolo a rottura dei ponti a volta sottile ed impalcato irrigidente. Giornale del Genio Civile, 1985, 11, 686-700.

[9]-Kang YJ, Scordelis AC. Nonlinear analysis of prestressed concrete frames. Journal of the structural division 106 ASCE 15191, 1980.

[10]-Kappos A, Penelis GG. Earthquake resistant concrete structures. Taylor & Francis, 1997.

[11]-Martinez y Cabrera F, Biondini F, Bontempi F, Malerba PG. Limit Analysis of Cable-Stayed Bridges. ICCCBE-VII, Seoul, Korea, August 1997, 431-436.

[12]-Martinez y Cabrera F, Biondini F, Bontempi F, Malerba PG. A Secant Technique for the N.L. Analysis of Prestressed Cable Stayed Bridges. ICCCBE-VII, Seoul, Korea, August 1997.

[13]-Massonnet CE, Save MA. Plastic analysis and design: beams and frames (Vol.1). Blaisdell Publishing Company, 1965.

[14]-Nielsen, MP. Limit Analysis and Concrete Plasticity. CRC Press, 1984.

[15]-Park R, Paulay T. Reinforced concrete structures. John Wiley & Sons, 1975.

[16]-Prager W. The theory of plasticity: a survey of recent achievements. Proceedings of the Institution of Mechanical Engineers, 1955, 41-57.

[17]-Quagliaroli M. From bidimensional towards monodimensional modeling of sound and damaged reinforced concrete structures. PhD Thesis, 2014.

[18]-Quagliaroli M, Malerba PG, Sgambi L. A parametric subdomain discretization for the analysis of the multiaxial response of reinforced concrete sections. Advances in Engineering Software 82, 2015, 87-104.